

WATER TUNNEL VISUALISATION AND NUMERICAL ANALYSIS OF FLOW AROUND TS-11 ISKRA WING WITH FLOW CONTROL SURFACES

Robert Szczepaniak, Szymon Walusiak, Robert Bąbel, Łukasz Mazurek

*Polish Air Force Academy, Aeronautics Faculty
Dywizjonu 303 Street 25, 08-521 Deblin, Poland
tel.: + 48 261 517 427*

e-mail: r.szczepaniak@wsosp.pl, r.babel@wsosp.pl, l.mazurek@wsosp.pl

Wit Stryczniewicz

*Institute of Aviation, Aerodynamics Department
Krakowska Av. 110/114, 02-256 Warsaw, Poland
tel.: +48 22 8460011 ext. 312*

e-mail: wit.stryczniewicz@ilot.edu.pl

Grzegorz Kowaleczko

*Air Force Institute of Technology
Ksiecica Bolesława Street 6, 01-494 Warsaw, Poland
tel.: +48 261 851 300*

e-mail: g.kowaleczko@chello.pl

Abstract

The article presents investigation of flow around wing of TS-11 Iskra airplane. The flow visualization around 3D printed model of wing with flow control surfaces was performed in a water tunnel. Two configurations were investigated: first with a flap and second with an aileron. The flow visualisation was performed with a use of a dye. The geometry of model was prepared with use Computer Aided Design (CAD) software basing on scans of real object and technical documentation. The model was built with use of additive manufacturing technology. Movement of the flow control surfaces was remotely controlled with servomechanisms incorporated in channels inside the model. In order to perform qualitative validation of the results the investigated flow was simulated with use of CFD commercial software. The article presents visualisation results of flow around wing section of TS-11 Iskra airplane and water tunnel model preparation. In order to perform qualitative validation of the results the investigated flow was simulated with use of CFD commercial software. The goal of the research was to investigate the complex flow field in the vicinity of flow control surfaces and provide aerodynamic characteristics at various deployment angles via numerical simulations. The results can be used for verification of water tunnel testing procedures and training.

Keywords: *flow visualisation, TS-11 Iskra aircraft, aileron, flap*

1. Introduction

Water tunnel testing has played a prominent role in understating of complex flow phenomena. These test facilities allowed to perform experiments in a systematic manner, playing a considerable role in formulating the most important theories of fluid mechanics. As an example, one can refer to works of Reynolds on flow turbulence [15, 16] or Prandtl on boundary layer theory [3]. Use of water tunnels allowed to develop empirical equations widely used in science and engineering.

The analogy of many flow phenomena in liquids and gases has grabbed the attention of early aerospace pioneers. Therefore, water tunnel tests were also introduced to aerospace testing procedures. The test in water was performed with use of balances [11] and flow visualisation of complex three-dimensional phenomenon [2, 10]. For example, the leading-edge extension was widely investigated with a use of water tunnels, which allowed developing next generation of combat planes.

Water tunnels are particularly suitable for use of three dimensional flow visualisation techniques. Historically, first flow visualisation with a use of dye was applied. An example of that kind of flow visualisation is presented in Fig. 1a. Advance of lasers allowed performing measurements that are more precise. The laser sheet was used to visualise the flow structures in well-defined position. The visualisation is perfumed by recording images of seeding illuminated with laser. Typically, aluminium particles are used [3]. The next step in was to come from qualitative flow visualisation to a quantitative measurements with use of image processing. Advance of Digital Particle Image Velocimetry (PIV) [4] allowed obtaining 2D vector velocity fields of flow in water tunnel in fast and accurate manner. Now, three dimensional measurement techniques are developed in order to provide volumetric velocity fields (for example systems from TSI – V3V (Volumetric 3 – Component Velocimetry) Fig. 1a or LaVision – Tomo-PIV).

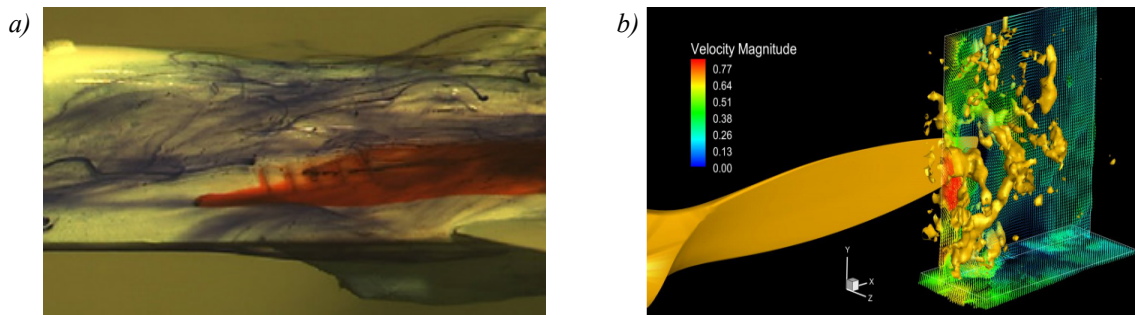


Fig. 1. Techniques of flow visualisation in water tunnel using: a) dye [14], b) V3V system [6]

Nowadays, more and more experimental water tunnel tests are replaced with use of Computational Fluid Dynamic (CFD) simulations [13], which has become the core tool in designing new planes and helicopters. Nevertheless, water tunnel test can provide many valuable data in cases where performance of CFD is still not fully trustworthy, like: high angle of attack [17] and flapping wing [18] aerodynamics.

The article presents results visualisation of flow around wing section of TS-11 Iskra airplane and water tunnel model preparation. In order to perform qualitative validation of the results the investigated flow was simulated with use of CFD commercial software. The goal of the research was to investigate the complex flow field in the vicinity of flow control surfaces and provide aerodynamic characteristics at various deployment angles via numerical simulations.

2. Wing of the TS-11 Iskra airplane

The skeleton of the wing consists of 15 ribs and many spars, which are the support for the metallic skin of the external surface. Inside the wing, there are located control systems for steering the aileron, flap and the aerodynamic brake as well as the hydraulic and electric installation elements. At the top side of the wing, along the rib between the aileron and the flap there is located an aerodynamic fence, which is used to provide the correct flow on the wing (Fig. 2a).

The TS-11 Iskra wing has the laminar profiles NACA 64 209 at the rib next to the fuselage and the symmetric profile NACA 64009 at the end of the wing [7, 8].

The metallic skin has double-slotted flaps. The flap is installed on the three trolleys guided on the arc-shape guides. Trolleys are attached to the flap edge by the levers. This kind of construction

ensures simultaneous exertion and movement of the flap, which leads to increase the wing chord as well as create two gaps between the flap and the wing. Starting position of the flap is 15 degrees and the landing position is 45 degrees.

TS-11 airplane is equipped with the non-slotted ailerons. Aileron has so called internal compensation, which reduces the hinge moment at the aileron steering system. It is the membrane located between the aileron and the special wall inside the flow. This special wall together with the wing metallic skin and the aileron edge form the compensation chamber. Aileron's trailing edge is doubled [10].

Under this work, preparation there was prepared model of the left wing of TS-11 Iskra (Fig. 2). The model was prepared using the SolidWorks software. The exact projection was possible thanks to the measurements made on the real model as well as the 2D technical documentation (rectangular views of the TS-11 Iskra wing) which was imported into the SolidWorks to ensure the proper contours of the wing.

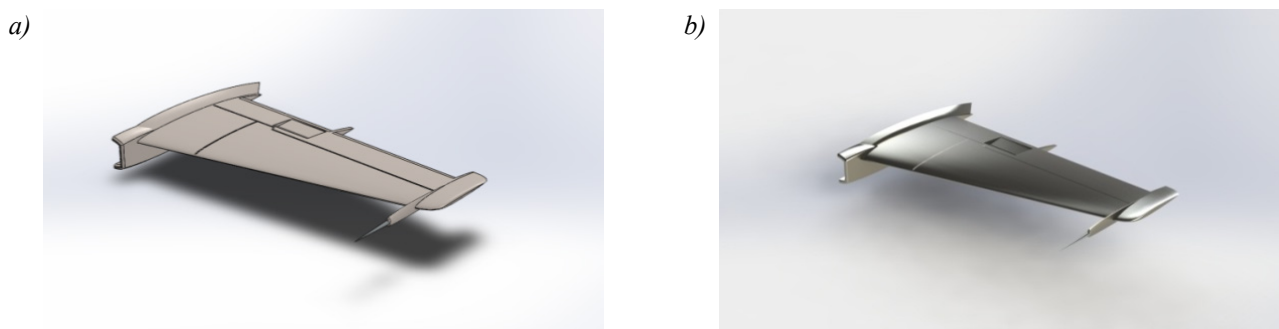


Fig. 2. Preliminary project of the wing ready for the 3D printing a) before rendering b) after rendering

However, because of the low 3D-printing efficiency it was impossible to exact project the wing geometry therefore it was decided to print only the some parts of the wing with aileron and flap, which were tested in the water tunnel.

3. Experimental verification

3.1. Preparation of the wing models with flap and aileron for the tunnel testing

At this stage of the design, process it was decided to not include the rounded fairing located at the end of the wing. In addition, an extra feature was added – aerodynamic fence – for more realistic wing definition comparing to the real model.

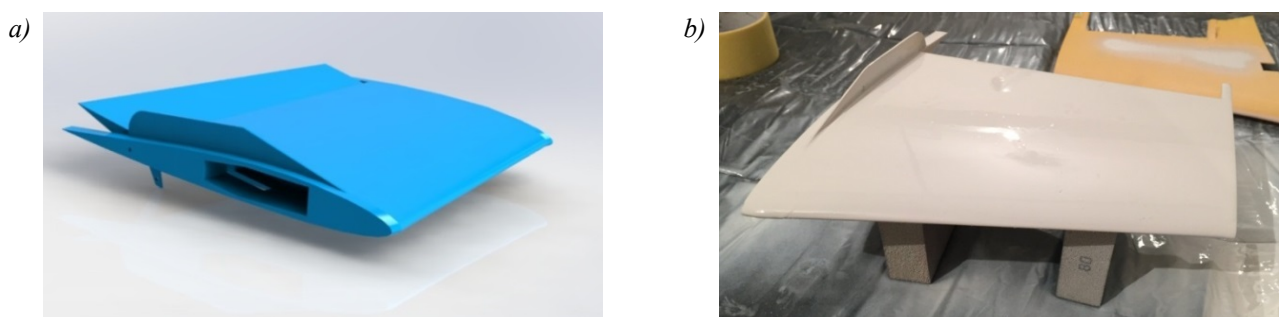


Fig. 3. The part of the wing with the aileron: a) in the SolidWorks environment after rendering, b) 3D printed model after manual correction

At the rear end of the model additional holes for the rod were made, which was guided also through the aileron. This rod is the rotation axis of the aileron. Additionally, there was designed

the guide for the aileron to provide the right aerodynamic compensation like the ones existing on the TS-11 Iskra wing.

An arm was designed in order to provide a connection between aileron, the pusher and the servomechanism. The complete model was connected during the assembly procedure and rendered to get high quality of the presented model (Fig 3a) as well as it was also printed and reworked by the model-making to ensure the highest possible surface roughness (Fig 3b).

In next stage of the research, it was decided to make the part of the wing with the double-slotted and movable flap. The main part of the wing (Fig. 4a) was built in such way to ensure the possibility to install servomechanism at the fuselage wing profile and the lever at the centre of the model. Additionally, extra cut was made at the bigger profile for the neodymium magnet. This magnet was used as the fixation of the model in the water tunnel.

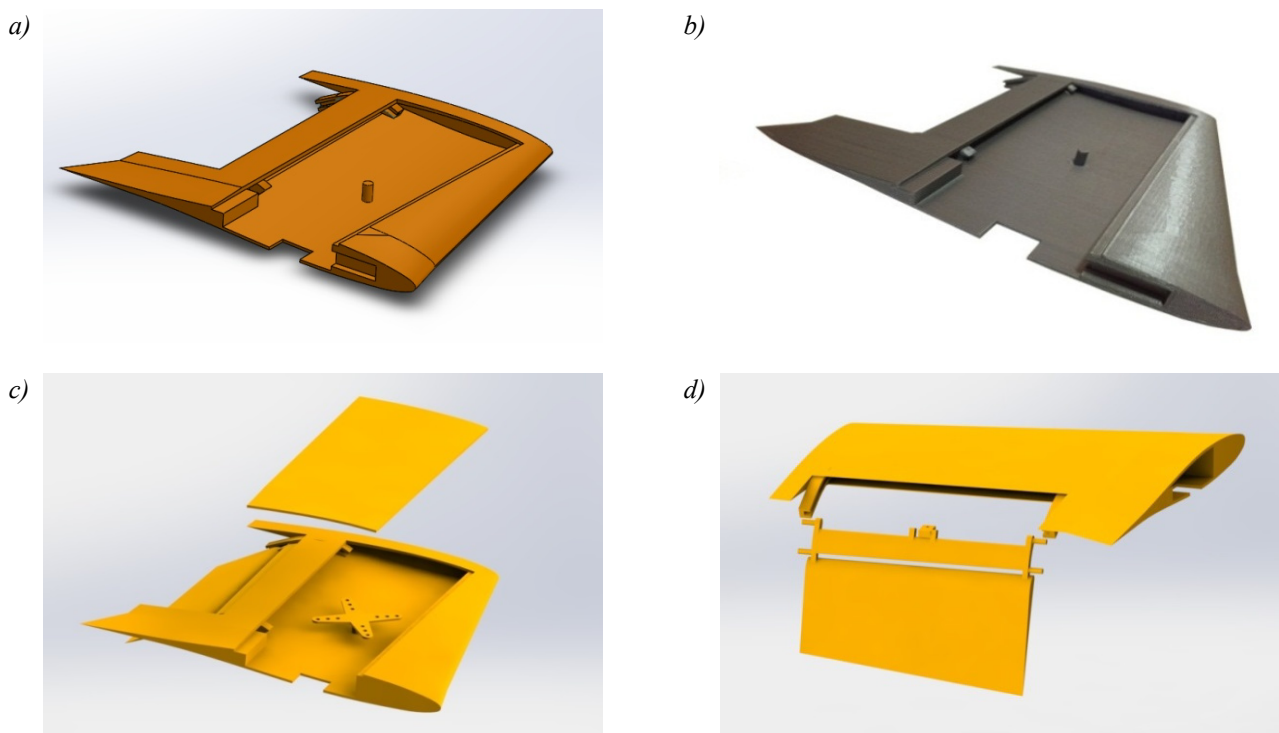


Fig. 4. The part of the wing with flap: a) main element, b) 3D-printed model, c) model with the double-slotted flap after the rendering with the view pointing to the angle-change mechanism, d) model with the double-slotted flap after rendering ready for the tunnel tests

The model of the movable flap (Fig. 4b) includes two pins guided on the both sides designed and 3D-printed model. They are responsible for keeping the flap in the guideway and maintaining the right angle during its exertion. In the middle of the model, there was installed connecting rod with the pusher elements. This mechanism ensures the movement with two degrees of freedom.

3.2. Test rig

Water tunnel, which was used during the practical tests, is the prototype (Fig. 5). The measurement capabilities range of this tunnel is the following:

- flow speed up to 15 cm/s,
- pitch angle within the range from -20 to $+45$ degrees,
- yaw angle within the range from -20 to $+45$ degrees.

Based on test requirements to check the influence of the wing mechanization system of the TS-11 Iskra airplane the yaw angle was setup every time to 0 degrees. The change of the pitch angle was done manually by using the neodymium magnet.



Fig. 5. Wing model prepared for the visualization test inside the water tunnel

For the flow visualization, it was used food colouring which was dosed by syringe and which was the mix of the red colour and orange [1].

3.3. Analysis of the experimental test results

The numerical model of the wing was used for the calculation using the classical $k-\epsilon$ turbulence model as well as with the Modified Wall Functions including the Van Driest's profile. The mesh used for the analysis was the rectangular parallel piped-shaped type (Fig. 6a) which consists of approximately 2.5 million elements. During the flow simulation, running it was assumed that the water is the fluid main medium with the following parameters: density 998.23 kg/m^3 and temperature 20°C . As the initial condition, it was assumed the flow velocity equal 4 cm/s , which are the real, value adequate to the water tunnel test conditions. The examples of the numerical calculations results are shown on Fig. 6b).

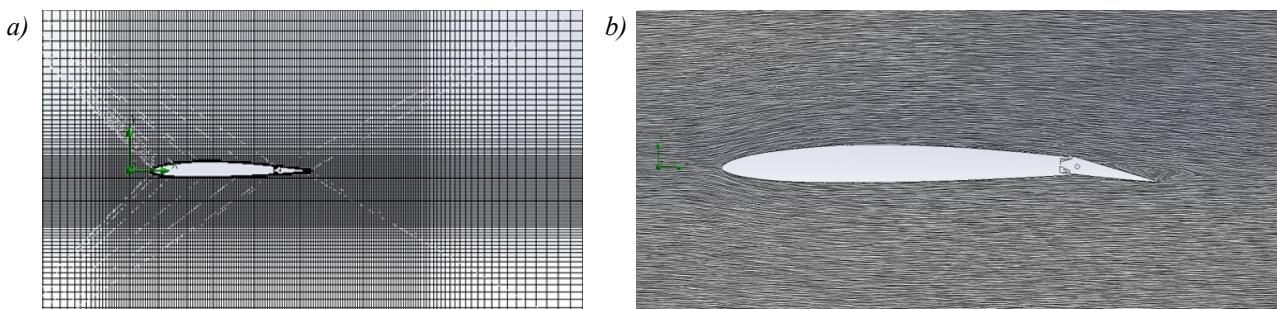


Fig. 6. a) Calculation mesh around the wing of the TS-11 airplane, b) examples of the calculation results

Results received based on the Solid Works flow simulation are the basis for the aerodynamic analysis of the wing. The scope of the simulation was focused mainly on the lift coefficient as well as the profile of modelled TS-11 wing.

Investigated airfoils were installed in the water tunnel and tested respectively. Flow visualization and numerical analysis were prepared for the angle attack equal 0 degrees and the aileron angles were equal: -10 , 0 and 10 degrees. Airfoil with the flap was tested for the angle attack equal 0 and 20 degrees where the aileron angles were 0 , 16 and 40 degrees. All the mentioned above attack angles were chosen based on each wing mechanization element used

during the flight manoeuvres. For each test variant, it was observed flow around the models for two water velocities: 4 cm/s and 8 cm/s.

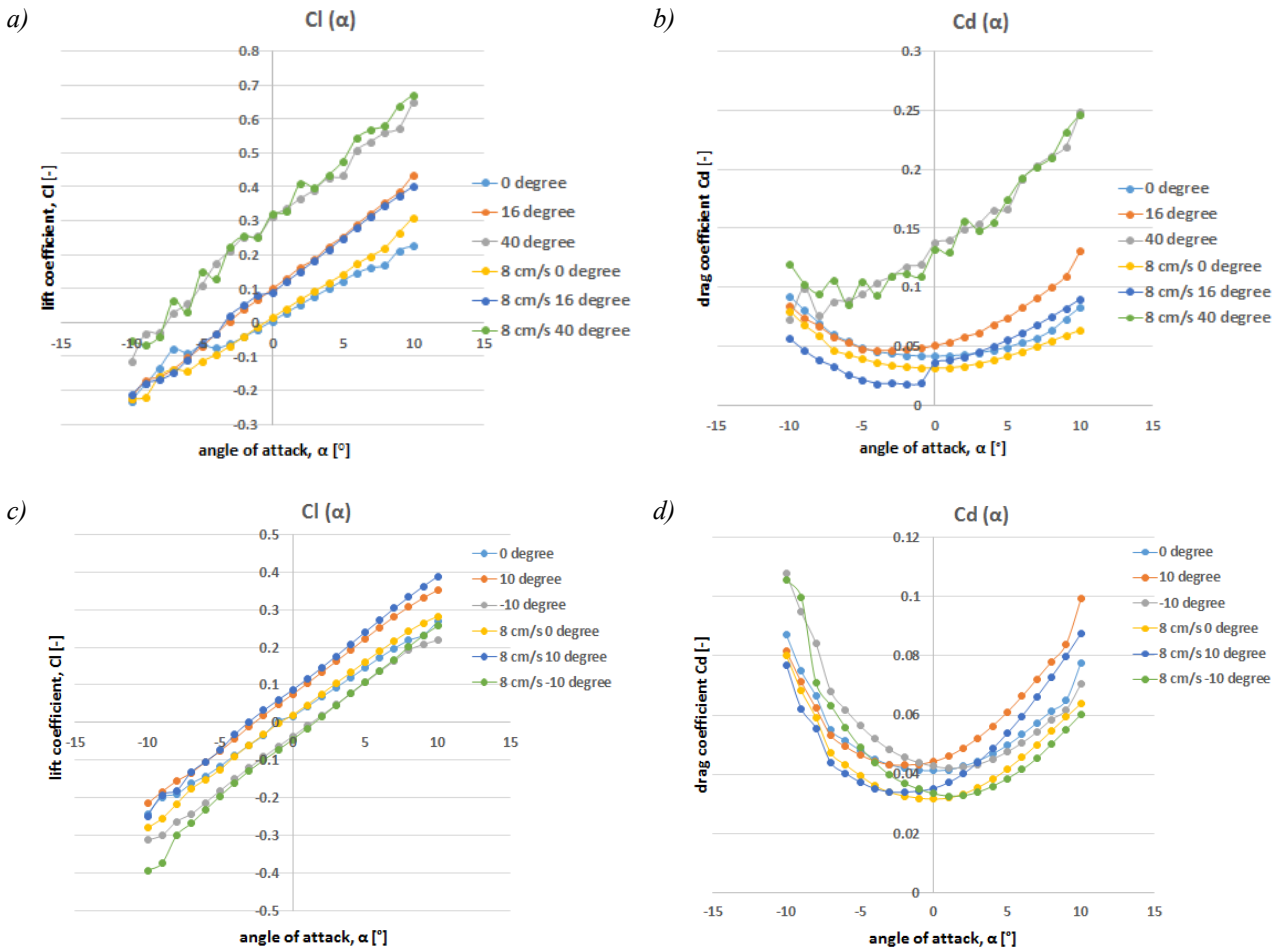


Fig. 7. Aerodynamic characteristics of the part of the wing: a) lift coefficient as the function of angle attack for the wing with the flap, b) drag coefficient as the function of angle attack for the wing with the flap, c) lift coefficient as the function of angle attack for the wing with the aileron, d) drag coefficient as the function of angle attack for the wing with the aileron

3.3.1. Numerical and experimental visualization of the wing model with the aileron configuration

As the first tested object, it was chosen the model of the wing with the aileron. All the observations were made for the flow speed equal 4 cm/s.

During the first test, the model was set up parallelly to the surrounding water streamlines and the aileron pitch angle was in the neutral position (Fig. 8a, b). There was observed at the whole profile length laminar flow of the dye, which flows parallelly to the profile curvature. After the aileron trailing edge, the turbulence occurs and the flow took the shape of the wave. Aerodynamic compensation of the aileron works correctly. During the test running, it was observed small violation of the dye streamline. It is caused probably by the small step, which was made during assembly of the components.

For the next test with the aileron pitch angle equal -10 degrees laminar flow was observed up to the joint between aileron and the profile. There was observed turbulence close to the trailing edge of the aileron, which transformed to the swirls (Fig. 8c, d). Similar effect (swirls appearing) is visible also for the profile with the pitch angle of the aileron equal 10 degrees. It is observed in visualization of both: water tunnel as well as the numerical calculation (Fig. 8e, f).

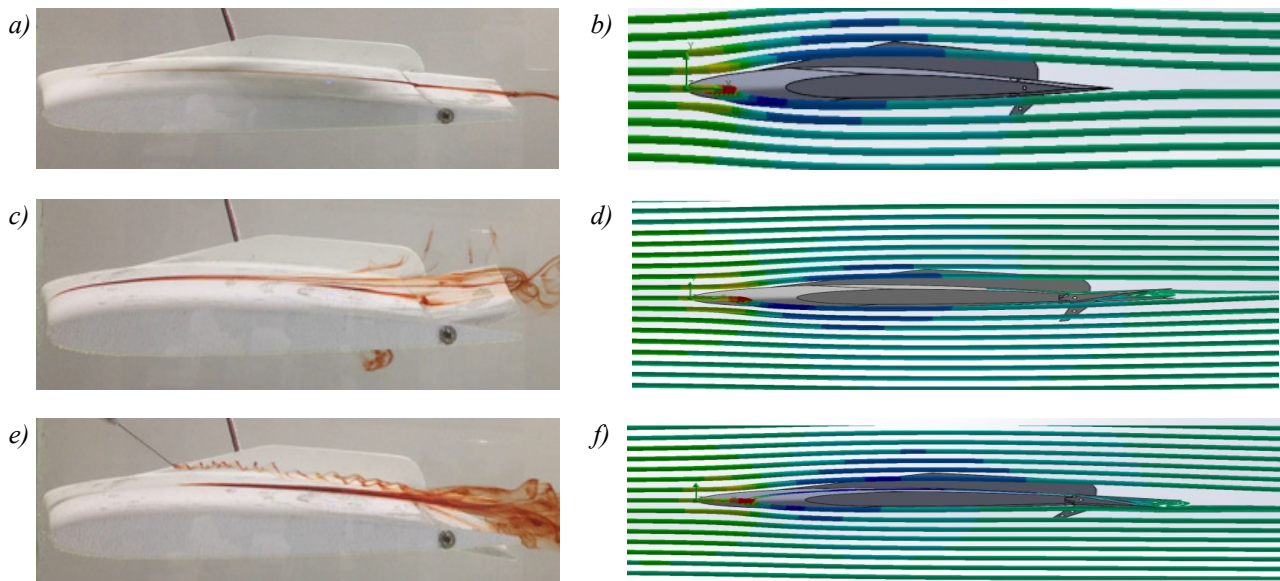


Fig. 8. Visualization and numerical results of the wing model with the aileron: a) flow around the model with the aileron, angle attack $\alpha = 0^\circ$, aileron pitch angle 0° , b) numerical visualization, c) flow around the model with the aileron, angle attack $\alpha = 0^\circ$, aileron pitch angle -10° , d) numerical visualization, e) flow around the model with the aileron, angle attack $\alpha = 0^\circ$, aileron pitch angle $+10^\circ$, f) numerical visualization

3.3.2. Numerical and experimental visualization of the wing model with the double-slotted flap configuration

The second part of the test considered the wing model with the angled and exerted double-slotted flap.

For the non-angled flap, it can be observed laminar flow around the complete chord of the wing model (Fig. 9a, b). At the next test, where the pitch angle of the flap was equal 16 degrees it is visible the transition between the laminar and turbulent flow at the place where flap is joined to the profile. Close to the trailing edge, the swirls occur caused by the flap exertion (Fig. 9c, d). The phenomena of the transition between the laminar flow and turbulent flow are also visible during the numerical calculations of the profile for the angle attack equal 20 degrees and for the pitch angle of the flaps equal 0 degrees. Turbulent flow occurs not far away from the leading edge (Fig. 9e, f). At the next stage for the angle attack equal 20 degrees and the pitch angle of the flaps equal 16 degrees similar phenomena occurs (swirls creation) like in the previous case. However, increasing the pitch angle of the flap causes also increase of the turbulence area around the profile (Fig. 9g, h).

4. Conclusion

Experimental test and numerical simulations showed qualitative similarity the results when one compare the images of flow visualisation with use of dye in water tunnel and streamlines plotted in the CFD software. The focal point of the research was to obtain information on the flow field in proximity of the control surfaces. The dye visualisation revealed location of flow separation. In order to obtain more detailed results two models for test in water tunnel was developed in a larger scale: one with a flap and one with an aileron. Model configuration was changed remotely.

The change of aerodynamic characteristics caused by flap and aileron deflection was confirmed by numerical simulations. This data are important for designer and pilots especially for low speed and high angle of attack phases of flight. Therefore, such numerical and experimental investigations are crucial part of development process of a new aircraft [12].

The presented results confirmed the feasibility of application of 3D printing technique for fabrication of models for water tunnel testing. Nevertheless, one should pay attention to the surface of the model after the printing process and take into consideration additional finishing in order assuring correct roughness. The model geometry and its surface needs to be tailored in order to meet requirements of tunnel testing (like similarity numbers).

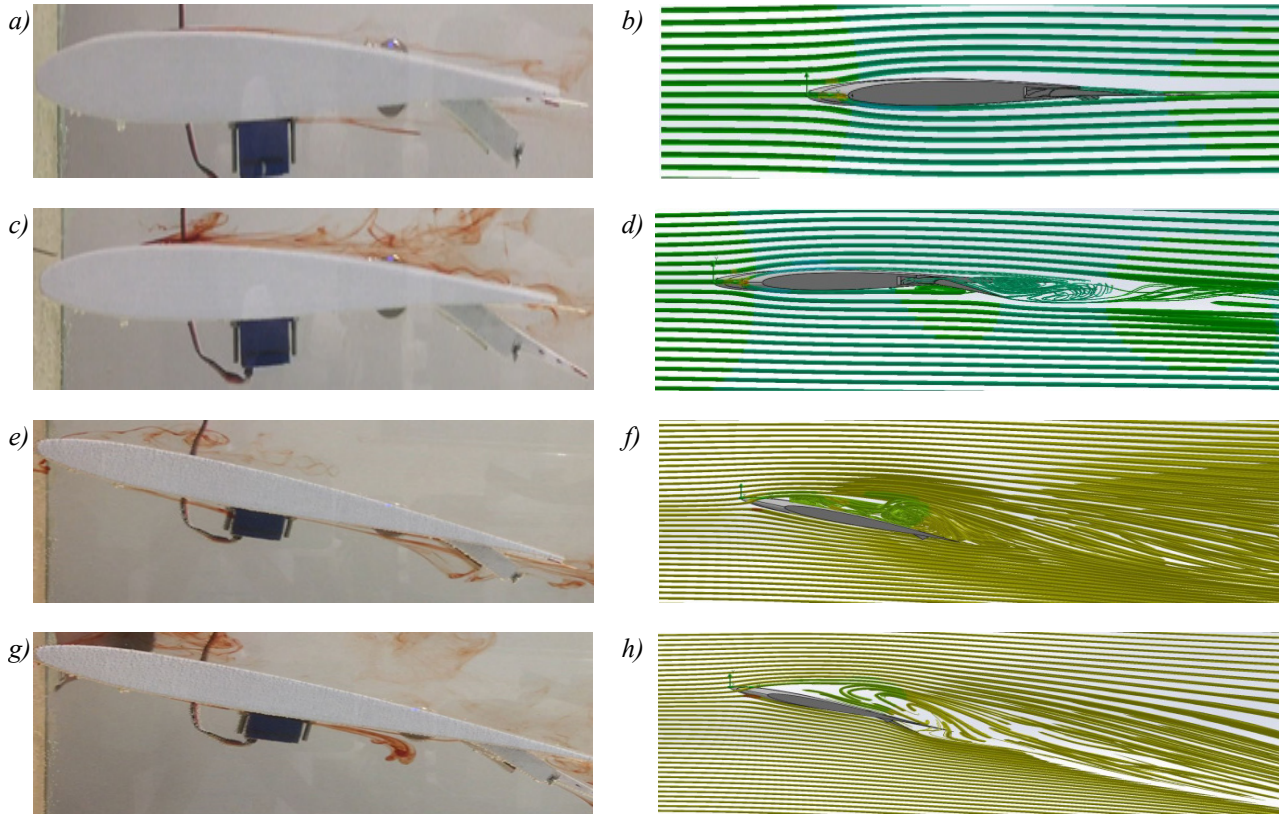


Fig. 9. Visualization and numerical results of the wing model with the flap a) flow around the model with the flap, angle attack $\alpha = 0^\circ$, flap pitch angle 0° , b) numerical visualization, c) flow around the model with the flap, angle attack $\alpha = 0^\circ$, flap pitch angle 16° , d) numerical visualization, e) flow around the model with the flap, angle attack $\alpha = 20^\circ$, flap pitch angle 0° , f) numerical visualization, g) flow around the model with the flap, angle attack $\alpha = 20^\circ$, flap pitch angle 16° , h) numerical visualization

References

- [1] *A hydrodynamic tunnel (prototype)*. Technical documentation TUN/2011, Project 122, ELBIT – An innovations-implementation company, 2011.
- [2] Erickson, G.,E., Peake, D. J., Del Frate, J., Skow, A. M., Malcolm, G. N., *Water Facilities in Retrospect and Prospect – an Illuminating Tool for Vehicle Design*, Tech. Memo. 89409, National Aeronautics and Space Administration, 1987.
- [3] Eckert, M., *The Dawn of Fluid Dynamics: A Discipline Between Science and Technology*, John Wiley & Sons, Weinheim 2006.
- [4] Stryczniewicz, W., *Algorytm do wyznaczania wektorowego pola prędkości metodą anemometrii obrazowej*, Problemy Mechatroniki, 9, pp. 41-54, 2012.
- [5] Merlo, N., Boushaki, T., Chauveau, C., De Persis, S., Pillier, L., Sarh, B., Gökalp, I., *Experimental Study of Oxygen Enrichment Effects on Turbulent Non-premixed Swirling Flames*, Energy Fuels, Vol. 27, pp. 6191-6197, 2013.
- [6] TSI, <http://tsi.com>.
- [7] Szkudlarz, P., *Analiza charakterystyk aerodynamicznych i osiągow samolotu TS-11 Iskra w oparciu o obliczenia inżynieryjne i wnioski z eksploatacji w powietrzu*, WSOSP Dęblin, pp. 12-14, 2003.

- [8] <http://m-selig.ae.illinois.edu>, dostępne w dniu 28.11.2016.
- [9] Kaczmarek, R., *Budowa i Eksploatacja samolotu TS-11 Iskra przez pilota*, Wyższa Oficerska Szkoła Lotnicza, pp. 43-45, , Dęblin.
- [10] Tennekes, H., Lumley, J. L., *A first course in turbulence*, MIT Press Design Department, pp. 59-74, USA 1972.
- [11] Barlow, J. B., Rae, W. H. Jr, Pope, A., *Low-Speed Wind Tunnel Testing*, John Wiley & Sons Inc., pp. 40, 1999.
- [12] Anderson, J. D. Jr, *Fundamentals of aerodynamics*, fifth editions in SI Units, McGraw-Hill, pp. 75-89, 2011.
- [13] Tucker, P. G., *Advanced computational fluid and aerodynamics*, Cambridge University Press, USA, pp. 386-403, 2016.
- [14] Filipiak, D., Szczepaniak, R., Zaorski, T., Bąbel, R., Stabryn, S., Stryczniewicz, W., *Flow visualization over an airfoil with flight control surfaces in a water tunnel*, Transactions of the Institute of Aviation, No. 1 (246), pp. 63-78, Warsaw 2017.
- [15] Rott, N., *Note on the history of the Reynolds Number*, Annul Review of Fluid Mechanics, 22, pp. 1-11, 1990.
- [16] Reynolds, O., *On the dynamical theory of incompressible viscous fluids and the determination of the criterion*, Philosophical Transactions of the Royal Society of London A, 186, pp. 123-164, 1895.
- [17] Smędra, K., Świerkot, R., Kubryński, K., *Low speed wind tunnel test of the jet trainer model at high angles of attack*, Journal of KONES Powertrain and Transport, Vol. 23, No. 4, pp. 471-478, 2016.
- [18] Sibilski, K., Pietrucha, J., Zlocka, M., *Comparative Evaluation of Power Requirements for Fixed, Rotary, and Flapping Wings Micro Air Vehicles*, AIAA Atmospheric Flight Mechanics Conference and Exhibit, 20-23 August Hilton Head, South Carolina 2007.

